Chapter 2

SELECTION OF REMOTELY SENSED DATA

Michael A. Lefsky[1,*] and Warren B. Cohen[2]
[1] *Oregon State University, Department of Forest Science, Corvallis, Oregon, 97331, USA*
[2] *USDA Forest Service, Corvallis, Oregon, 97331, USA*

1.   INTRODUCTION

An increasing number of sensors are available for forest ecologists and managers seeking to map attributes of forest canopy cover, forest structure and composition, and their dynamics. This Chapter seeks to put these advances within the context of the needs of forest managers and scientists. To do so, we review the basic physics behind a variety of imagery types, discuss fundamental limitations and trade-offs that apply to all remotely sensed data, review sensor options for several established and emerging technologies, and present our approach for matching imagery and attributes of interest.

2.   PARAMETERS OF IMAGE CREATION

The choices involved in the selection of a remote sensing data type are increasingly complicated. Images may be created using active or passive techniques, in optical or microwave wavelengths, and with ranging techniques like LIDAR (light detection and ranging) or IFSAR (interferometric synthetic aperture radar). Nevertheless, the spatial, spectral, radiometric and temporal resolution of the imagery remains key to their

* Current affiliation: Department of Forest Sciences, Colorado State University, Fort Collins, Colorado, 80523-1470, USA

utility for the user. Furthermore, trade-offs between these resolutions, the extent of the imagery, and other sensor particulars are often key elements of designing a remote sensing solution.

2.1   Modes of image formation

While it is tempting to resort to the familiar example of photographs when viewing remotely sensed images, it is important to remember that only conventional optical remote sensing is clearly analogous to photography; the physical processes involved in radar or lidar remote sensing are quite unlike the familiar interaction of light with either the human eye or camera. Radar, in particular, behaves in ways outside the common sense experience of non-specialists. It is therefore important to review the physical bases of each sensor.

2.1.1   Optical images

Optical images have been, and will likely continue to remain for some time, the most frequently used type of remote sensing. In this Chapter, optical denotes that the medium (analog or digital) is sensitive to light in the range of 400 nm (nanometers, i.e., violet), to 2500 nm in the shortwave infrared (Colour Plate 1). From 2500 nm to 14,000 nm is the thermal range of the electromagnetic spectrum, in which most radiation observed by sensors has been emitted from the Earth's surface, not from the Sun. While thermal remote sensing can be very important for certain kinds of natural resource investigations, including geological mapping (Abrams et al. 1984; Mouginis-Mark et al. 1994), estimation of plant-canopy temperatures (Sader 1986; Luvall et al. 1991), and prediction of runoff from snow pack, it is beyond the scope of this discussion, as these are of secondary interest to the forest ecologist and manager. The optical range of wavelengths is important for remote sensing of vegetation because the majority of the Sun's energy is emitted in this range, and plants have become adapted to either absorb (e.g., for photosynthesis) or reflect (e.g., to maintain their heat balance) at various wavelengths (Gates 1952). Although optical images can be created using an independent source of energy, such as a flash lamp, they are normally created passively, using the Sun as a source of energy, and therefore, to adequately understand these images, we will have to start with the quantities and qualities of energy emitted by the Sun.

The bulk of solar radiation at the top of the atmosphere is distributed above 200 nanometers (in the ultraviolet), with peak strength at 500 nm (in the visible), and thereafter declining so that by 2500 nm (in the shortwave infrared) it has roughly one-twentieth of its peak power (Colour Plate 1- top

panel). However, the output of the Sun is only the first part of the story, because the atmosphere is not uniformly transmissive to energy at these wavelengths (Colour Plate 1, top panel). The sharp atmospheric absorption features (e.g., at 940 nm) are due to molecular absorptance by CO_2 and H_2O in the atmosphere, even under clear sky conditions (Schowengerdt 1997). As important as these individual features are, it is the general pattern of decreasing transmittance from 1200nm to 400nm, due to scattering by air molecules themselves, as well as by aerosols and other particulates, that plays a more important role in the atmosphere's effects on optical images.

Beginning at the top of the atmosphere, most solar radiation takes one of three paths to an optical sensor (Schowengerdt 1997). *Unscattered, surface-reflected radiation* passes through the atmosphere without being intercepted, will interact with the surface, and be reflected back to the sensor. *Scattered, surface-reflected skylight* will encounter one or more scattering events in the atmosphere that deflects the light into target pixel, where it will be reflected in the direction of the sensor. *Path radiance* consists of radiation that encounters one or more scattering events in the atmosphere, and is reflected back up in the direction of the sensor, without having reached the surface.

Reflectance is the physical interaction between solar radiation and the Earth's surface that gives rise to the spectral information content of an optical image. Energy is reflected from surfaces in what is often considered to be a spatially uniform (or Lambertian) manner but is in fact a complex pattern that is dependent on illumination and view angle and surface roughness; this pattern is referred to as the bi-directional reflectance distribution function or BRDF (Kimes et al. 1993; Ranson et al. 1994; Asner et al. 1998). More relevant for the applications-oriented user of optical imagery is the spectral variability of reflectance. As shown in Colour Plate 1 (middle panel), plants tend to exhibit a number of common features, including low reflectance in the visible spectral range (especially in the blue and red wavelengths), a steep increase in reflectance around 700 nm (the so-called red-edge) and high reflectance in the near-infrared. While many minerals have sharp spectral features, spectra that are distinct from other minerals, and often occur in isolation over large areas, most species of plants have similar spectra and tend to be mixed at the sub-pixel level with other spectra, such as soil and shadow (Li and Strahler 1992; Cohen et al. 1995). As a consequence, discrimination of physiognomy and species from optical imagery is problematic.

After reflecting off the target, radiation proceeds back through the atmosphere (where once again it may be intercepted by the atmosphere) and then to the sensor, where it is either recorded as an arrangement of differentially exposed halide crystals (as in Hall, Chapter 3), or as a set of digital numbers of a given precision. Both airphotos and digital images

record energy properties at a point in time for a portion of the Earth's surface. Using different combinations of film sensitivity and filters, airphotos can selectively record certain wavelength ranges of the electromagnetic spectrum. Digital sensors also use filters, but in lieu of using halide crystals in a film emulsion to record the image, they use energy detectors that are similar in concept to voltmeters. Energy incident upon a detector is converted to a digital number, commonly 8-bit, but often 9-, 10-, 12-, or 16-bit. Normally, one detector is dedicated to a single wavelength range, and multiple ranges are sensed using multiple detectors. Whereas photographic film is limited in sensitivity to a narrow range of the electromagnetic spectrum (400-900 nm), digital optical sensors can operate in a much wider range of the spectrum (400-14000 nm, Lillesand and Kiefer (2000)).

At any wavelength the power of the recorded signal is due to the entire series of conditions discussed thus far; the irradiance of the Sun at the top of the atmosphere, the transmittance and scattering by the atmosphere, and the reflectance of the target, all of which vary as a function of wavelength, topography and BRDF effects. Of these, only reflectance and it variation expressed in the BRDF, are properties of the vegetation, and they are the quantities that most remote sensing analyses strive to extract from the at-sensor radiances recorded by either film or digital sensors. The process of deriving reflectance is discussed in detail in Peddle et al. (Chapter 7).

2.1.2   SAR images

Whereas most optical images are collected passively, most microwave images are collected actively, with the device providing the energy illuminating the scene and collecting the backscattered radiation from the target (passive microwave devices, while useful for sea ice detection (Eppler and Farmer 1991), airborne water vapor, and some soil moisture measurements (Chauhan 1997), are again outside the purview of this discussion). Active sensors can operate without concern for the Sun's illumination angle and can even be flown at night. The most common implementation for microwave sensors is synthetic aperture radar or SAR. As in the optical spectrum, varying microwave wavelengths have been established as being particularly useful for different purposes. However, the illumination from microwave sensors generally has a wavelength of 1 mm to 1 m, about two thousand to two million times the wavelength of green light (500 nm). As a consequence, the physical interaction of microwave illumination with forests is very different from that in the optical range. Whereas pigments, leaf structure, and leaf water content reflect optical radiation, and patterns of foliage and shadow allow the prediction of

structure; the microwave portion of the spectrum is directly sensitive to the structure of the forest itself, with each microwave band being preferentially backscattered by objects of approximately the band's wavelength (Ranson and Williams 1992). Radar in the shorter wavelengths (X and C, see Figure 2-1), are sensitive to small twigs and leaves, while long wavelength bands (L and P) are sensitive to boles and branches. Therefore, shorter wavelength bands are most sensitive to the uppermost canopy level, while longer wavelength bands penetrate the upper canopy and provide information on the woody structure and underlying ground surface. An additional feature of microwave sensors is that they can be configured to send and receive signals in a vertical (V) or horizontal (H) direction. Combining these send and
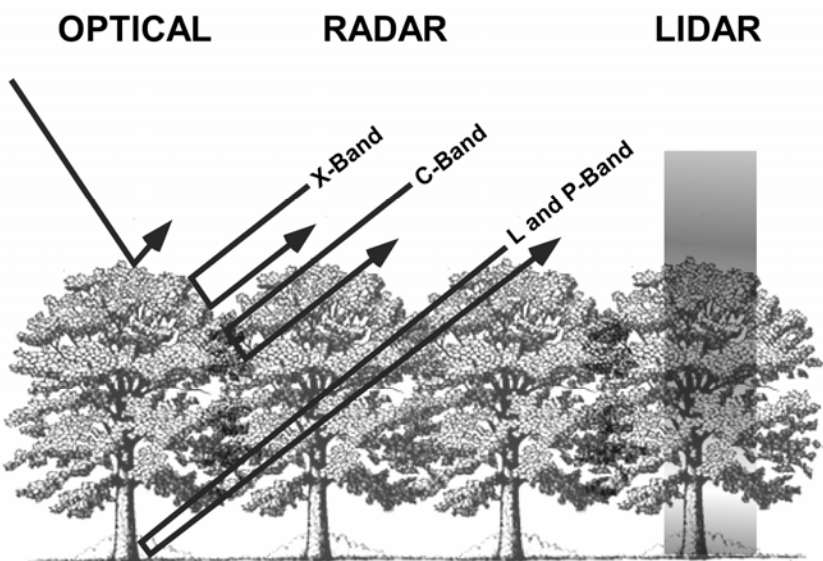
Figure 2-1. Diagram indicating the conceptual differences in the depth to which various sensors will penetrate into the forest canopy, indicating the ability of L- and P-band radar to penetrate leaves and twigs, and only be reflected by larger structures. Lidar is an optical instrument, but due to the ability to track the depth of penetration through open spaces in the canopy, information concerning sub-canopy features can be recorded.

receive options, quadruple polarized sensors can use all four combinations (HH, VV, HV, VH) to accentuate the backscatter from features with particular orientations, such as tree boles in a recent clear cut (Kasischke et al. 1994). One clear advantage that microwave sensors hold over optical remote sensing is the transparency of the atmosphere, and atmospheric aerosols, in the microwave portion of the spectrum. This allows SAR to be used during cloudy or smoke-filled conditions when optical remote sensing would be useless or nearly so. As a consequence, microwave instruments

have been extensively used in the tropics (Luckman 1998) and in the higher latitudes (Kasischke et al. 1994), where cloud free conditions are rare.

In addition to being sensitive to vegetation structure, a surface's inherent reflectivity in the microwave is determined by its dielectric constant, which governs electromagnetic wave propagation. In vegetated areas, the moisture and freeze-thaw state of the ground and canopy surfaces predominantly determines this constant. This phenomenon has been used to map freeze-thaw conditions (Rignot and Way 1994; Rignot et al. 1994; Way et al. 1994), water stress in trees (Way et al. 1991), and, in the absence of appreciable biomass, can measure soil moisture in the upper 10 cm of the soil profile (Dobson et al. 1992; Wang et al. 1994). In addition, the combination of open water and standing vegetation (e.g., in flooded areas with either trees or other vegetation with an upright orientation, such as reeds) results in an extremely high backscatter, making these areas easy to detect. While this dielectric effect can be useful for hydrological and freeze/thaw mapping, this phenomenon can also interfere with the remote sensing of vegetation structure, if moisture conditions are not uniform across the area of interest.

A recent innovation in microwave remote sensing is the technique of Interferometric SAR (IFSAR). IFSAR uses two radar receivers separated in space, and measures the difference in signal phase between the two return signals to estimate the three-dimensional position of the mean scattering elements (Baltzer 2001). In some applications, a single microwave sensor makes the IFSAR measurement by recording two images of the same area from different orientations, sometimes at different times (repeat pass interferometry). The primary use of this technology is topographic mapping, as with the Shuttle Radar Topographic Mission (SRTM, Eineder et al. 2000). In addition to producing topographic information, the strength of the correlation (coherence) between the two IFSAR return signals is affected by the presence of volumetric scattering, such as occurs in vegetation canopies, as first pointed out by Rodriguez and Martin (1992). The estimation of canopy structure parameters from a single interferometric measurement relies on assumptions about the canopy structure, such as the canopy dielectric properties. An alternate approach that has been used successfully is the joint use of lidar and interferometric data to retrieve canopy parameters from the IFSAR data (Rosen et al. 2000; Rodriguez et al. 2002).

2.1.3   Lidar remote sensing

Laser altimetry, or lidar is an alternative remote sensing technology that directly measures the three-dimensional distribution of the plant canopy and sub-canopy topography. The basic measurement made by these devices is the distance between the sensor and a target surface, made by determining

the elapsed time between the emission of a short-duration laser pulse and the arrival of the reflection of that pulse (the return signal) in the sensor's receiver. Dividing this time interval by the speed of light results in a measurement of the round-trip distance traveled, and dividing this distance by two results in the distance between the sensor and the target (Bachman 1979). Key differences among lidar sensors are related to the wavelength, power, pulse duration, size, divergence, and repetition rate of the laser itself; the size and spacing of the laser-illuminated samples on the ground, and the information recorded for each reflected pulse. Lasers for terrestrial applications generally have wavelengths in the range of 900-1064 nm, where vegetation reflectance is high (compared with the visible wavelength (400-700) where absorptance is high and little signal would return from the surfaces). Early lidar sensors were profiling systems; recording observations along a single narrow transect. Later systems operated in a scanning mode, in which the orientation of the laser illumination and receiver field of view was directed from side to side by a rotating mirror, or mirrors, so that as the plane moved forward, the sampled points fell across a wide band or swath. It must be noted that, unlike optical or microwave remote sensing, lidar produces swaths of points, not images. However, these can be used to create gridded coverages that resemble images, after appropriate post-processing.

The intensity or power of the lidar return signal is limited by several factors: the total power of the transmitted pulse, the reflectance of the intercepted surface at the laser's wavelength, the fraction of the laser pulse that is intercepted by a surface, and the fraction of reflected illumination that is scattered in the direction of the sensor. The laser pulse returned after intercepting a morphologically complex surface, such as a vegetation canopy, will be a complex combination of energy returned from surfaces at numerous distances, the distant surfaces represented later in the reflected signal (Harding et al. 2001). The type of information collected from this return signal distinguishes two broad categories of sensors. *Discrete-return* lidar devices measure either one (single-return systems) or a small number (multiple-return systems) of heights by identifying, in the return signal, major peaks that represent discrete objects in the path of the laser illumination. The distance corresponding to the time elapsed before the leading edges of the peak(s), and often the power of each peak, are typical values recorded by this type of system (Wehr and Lohr 1999; St. Onge et al., Chapter 19). *Waveform-recording* devices record the time-varying intensity of the returned energy from each laser pulse, providing a record of the height distribution of the surfaces intercepted by the laser pulse (Harding et al. 2001; Lefsky et al. 2002). Both discrete-return and waveform recording sensors are typically used in combination with instruments for locating the return signals in three dimensions.

2.2   General characteristics of imagery

There are four general concepts that apply, with slight modifications, to sensors in all three of the modes of image formation we have discussed (i.e., optical, microwave, and lidar). These are: spatial resolution and extent, spectral resolution, radiometric resolution, and temporal resolution and extent.

2.2.1   Spatial resolution and extent

Spatial resolution, commonly referred to as "pixel size" in digital images, is a key element of both digital and airphoto remote sensing. Airphotos have an inherent spatial scale that is a function of camera focal length and aircraft flying height. Although photo scale can be thought of as related to the unit area of the Earth's surface that can be resolved, resolution of airphotos is also a function of the film's halide crystal grain size (or film speed). Digital sensors also have inherent spatial properties, but rather than referring to scale, the term spatial resolution or pixel size is most commonly used. Digital image spatial resolution refers to the size of the individual physical sample unit on the ground that is sensed by a given detector at any instant in time. For example, a resolution of 10 m means a single digital cell contains integrated spectral information from a nominal 10 m x 10 m unit of the Earth's surface. In practice, the design of a sensor can allow the energy that is recorded for a single pixel to come from beyond that pixel's nominal boundary, but this is rarely an issue in applications.

The spatial resolution of lidar data cannot be summarized in a single pixel size as can be done for optical and microwave images. For these latter images types, data is usually collected such that the instantaneous field of view (IFOV; the area over which each pixel integrates) approximates the spacing between adjacent pixels. For airborne discrete-return lidar, measurements are usually made in a Z-shaped or sinusoidal path as the platform moves forward. The IFOV of an individual measurement is determined by the divergence of the (initially narrow) laser beam, and the altitude above ground level of the platform. The lidar IFOV for forested areas is usually less than a meter, while the spacing between measurements is generally a meter or more, therefore the coverage of the scene is not spatially comprehensive. However, these spot measurements of height can be processed to a gridded image of the maximum height surface (Digital Surface Model), minimum height surface (Digital Terrain Model), or an image of canopy height above the terrain. Waveform recording lidar uses large footprints that are contiguous, and the concept of spatial resolution applies as it would for conventional optical sensors. However, these sensors

add a vertical component to spatial resolution, as their measurements are made using vertical bins of specified depth within each pixel (Harding et al. 2001).

Users of remote sensing data have developed a common frame of reference for efficient and effective communication, starting with the taxonomic structure for remote sensing models developed by Strahler et al. (1986). This taxonomy distinguishes between a ground scene and an image of that scene, the continuous versus discrete nature of a scene, image spatial resolution and scene object resolution, and deterministic and empirical models of a scene. Concepts associated with scale and spatial resolution in relation to image processing models are further developed by Woodcock and Strahler (1987). This paper is required reading for anyone faced with a choice of image data and processing schemes for a specific set of mapping objectives. What Woodcock and Strahler (1987) demonstrate is that the spatial structure of a scene in combination with the type of information desired from associated imagery, tend to limit the choice of appropriate image processing models for classification (e.g. spectral classifiers, spatial classifiers, mixture models, and texture models). Together, these two seminal papers provide a foundation from which to build a solid understanding of the spatial aspects of remote sensing.

2.2.2   Spectral and radiometric resolution

Spectral resolution is a complex attribute that refers to both the number and spectral width of the bands in a given sensor. Sensors with more bands and narrower spectral widths are spoken of as having higher spectral resolution. The spectral resolution of most current operational remote sensing systems is quite limited. Landsat TM has six spectral bands in the reflective portion of the electromagnetic spectrum and one in the thermal-infrared region. SPOT HRV multispectral imagery consists of only three spectral bands. Hyperspectral data (e.g., instruments with more than 200 narrow spectral bands) is becoming more widely available (Vane and Goetz 1993), but is not yet at the stage where satellite data can be ordered, although this may change in the next few years.

For microwave, spectral resolution refers both to the number of bands available, and because of their ability to increase the utility of the data, the number of polarization combinations that can be used. Terrestrial lidar sensors have, until recently, used only a single spectral band, most often between 900 and 1064 nm. Bathymetric sensors have long used two wavelengths, one to determine the height of the water surface, another to penetrate it. Bathymetric sensors have been used in terrestrial applications (Nilsson 1996), with improved discrimination of the foliage and ground

surfaces. However, there are now emerging plans for several multispectral lidar devices, including NASA's Experimental Advanced Airborne Research Lidar (EAARL, Brock and Wright 2000).

Radiometric resolution is often interpreted as the number of intensity levels that a sensor can use to record a given signal. In an optical sensor this signal is the at-sensor radiance, which is commonly quantised to 8 bits. This gives the sensor 256 grayscale levels to record a given signal. However, many sensors use 10 or 16 bits to record a given signal, yielding 1024 or 65536 levels of gray respectively, thus allowing finer discrimination of the radiance at a particular wavelength.

2.2.3   Temporal resolution and extent

Temporal resolution, often referred to as the "revisit interval", is the time between opportunities to obtain imagery over a given spot. Temporal resolution is a key attribute even when only one image is required, especially when adverse atmospheric conditions are in place during much of the time when one wishes to obtain imagery. The probability of obtaining an image with clear sky conditions in a place like the Pacific Northwest of the U.S. or the Brazilian Amazon is directly related to the number of viewing opportunities, and therefore to temporal resolution. While one image per area of interest is the norm for most studies, the ability to capture phenological changes (Townsend et al 1985; Oetter et al. 2000) and, in passive optical images the changing interaction of the Sun with the geometry of a forest canopy, can lead to substantial improvement in the prediction of forest attributes (Wolter et al. 1995; Lefsky et al. 2001).

Temporal extent is an often-overlooked aspect of sensors. Normally, we look for an optimal sensor in terms of its ability to meet our current needs. However, many forestry applications have, or will develop, a significant historical component. This fact should be considered when designing a remote sensing project. For instance, the MSS is a four-band sensor with an unusual rectangular pixel that is 57 m x 80 m. For most applications, images from the TM sensor have replaced it. However, MSS has one attribute that no other sensor can ever match – it was the first moderate-resolution, multispectral, digital satellite sensor. If you need to map forests in the years between 1972 and 1983, or assemble (in the year 2002) a 30-year record of forest change, you will need to work with MSS, and consider how to compare it to more modern imagery types (Franklin et al., Chapter 10). Similarly, if there is likely to be a continuing demand for work in the study area, the ability to collect similar imagery at a later time should also be considered.

2.3 Sensor tradeoffs

Three sensor tradeoffs need to be discussed before a brief review of commonly used sensors is made. These tradeoffs include the use of a sensor on an airborne or satellite platform, the use of digital or analog image collection and processing, and the tradeoff between the various types of resolution and image extent.

2.3.1 Airborne versus satellite

Trade-offs between airborne and satellite image collection include both practical logistical tradeoffs and fundamental tradeoffs in the kinds and quality of data that are available. At the most practical level, most satellite collections of data are available only on predetermined schedules, and even those with an "on-demand" capability are also limited by their orbits and the demands of other users. In contrast, airborne data collections usually offer a much greater level of flexibility. An airborne system can wait for better weather conditions (although that may be costly), whereas a satellite may not be overhead for weeks-- at which time the phenomenon you want to view may be gone. Airborne systems can also sample at any time of the day (and sometimes night) whereas satellites generally pass over a site at the same time each day. Airborne sensors can wait for clouds to clear, or to fly the cloud-free areas of a large area until the project is completed. In addition, many missions are simply flown below the altitude of the clouds that would show up on a satellite image.

An additional set of advantages of airborne data result from the relative ease with which sensors can be fitted in an airborne platform, as opposed to being launched on a satellite. As a consequence a wider, and more technologically advanced, set of sensors is available for airborne platforms. These sensors include systems with higher spectral resolution, and advanced microwave and lidar sensors, many of them "proof-of-concept" devices for what (we hope) will be future satellite systems. Of course, higher spatial resolutions are easier to obtain from airborne platforms, due to their lower altitude.

While airborne sensors have their advantages, it is generally satellite systems that have the most advantages for the scientist or manager interested in understanding, mapping and managing large areas. Landsat TM and ETM+ images, one of the most widely used types of imagery, are each 185 km wide by 185 km long, and are taken at an altitude of 705 km. In the absence of clouds or haze, that entire area will be radiometrically consistent, and can in some cases be analyzed with only a few preprocessing steps. In contrast, images collected from an airborne platform will require radiometric

correction and mosaicking before they can be used. In addition, geometric distortions due to topography are less pronounced in imagery collected at higher altitudes, making the satellite images easier to geo-register.

2.3.2   Digital versus analog

Given the recent emergence of high spatial-resolution digital sensors on both satellite and airborne platforms, and our general eagerness for new technology, it would seem that airphotos would gradually be phased out of forest remote sensing. Nevertheless, they retain a number of advantages over digital sensors. Aerial photography is the oldest, most frequently used, and best understood form of remote sensing. The spatial resolution of aerial photographs is variable, but high-resolution aerial photography has the best spatial resolution of all remote sensing techniques. For forestry applications, a moderate resolution photo would have a 1:12000 scale, equivalent to a spatial resolution of about 0.4 m. Higher resolution aerial photography (1:5000), would have a spatial resolution of about 0.16 m, and could be used for mapping of forest regeneration and similar purposes (Pitt et al. 1997). Digital frame cameras or satellite sensors such as IKONOS cannot currently match this level of spatial resolution at the swath widths available with aerial photography.

The advantage of digital images is that they are ready to be used with *image processing* software, allowing a number of automated enhancement and classification procedures to be applied. In contrast, *image interpretation* generally requires an experienced specialist, using manual procedures, to extract forest inventory information, and as a result the interpreted information can be expensive, time-intensive, and may vary from one interpreter to another (Wulder 1998). As a consequence, digital methods have been introduced in an attempt to expedite the photo-interpretation process and make it more consistent. However, interpretation is often still necessary, and in some cases cost-effective, for extracting those forest stand attributes that rely on sophisticated identification of subtle spectral and textural signatures.

2.3.3   Resolution versus extent

We have discussed four types of resolution- spatial, spectral, radiometric and temporal. All else being equal, we might prefer to address our remote sensing problems using images with small pixels, a large number of spectral bands, and with multiple images taken closely in time. However, there is a drawback to such a strategy – we cannot increase any of these resolutions without increasing the quantity of data collected. While processor speed and

storage capacities seem to be increasing without end, our on-going informal survey of remote sensing labs suggests that the volume of data they are processing is increasing as fast or faster than improvement in the technology. Fortunately, the optimal resolution for a given application is hardly ever the maximum available resolution.

2.3.3.1 Spatial resolution

Spatial resolution, as discussed by Strahler et al. (1986), can be best understood in reference to the size of the objects that we want to sense. Imagery whose spatial resolution is coarser than these objects are low, or L-resolution. The radiance of image pixels of this type is a function of multiple objects (including background), and this averaging effect can be useful by reducing high spatial frequency variance. This is useful, for example, in that it creates the kind of stable and representative spectral classes needed for many types of image processing. However, when pixels are much larger than the objects of interest, they will tend to average multiple objects that have different attributes. In contrast, high, or H-resolution, images will contain multiple pixels for each object, which adds to the overall variance of the image. For instance, in an image in which individual trees are represented by multiple pixels, each pixel may be shadowed or sunlit, young foliage or old, or may contain one of a variety of different understorey components. If one is going to map forest as a single class, rules will need to be developed to incorporate all of these cover types into one, and also to separate, for instance, shadow in the forest from shadow on the shoulder of a road (Culvenor, Chapter 9). As a consequence, images with a spatial resolution near the size of the objects of interest are usually preferred (Woodcock and Strahler 1987).

One successful strategy that numerous researchers have pursued is the combination of high and moderate (or moderate and low) spatial resolution data. Cohen et al. (2001) used aerial photography to visually estimate total and coniferous tree cover, and visual crown diameter, for photo-plots over western Oregon, which could be done reliably and did not require expensive fieldwork. They then used regression between this data and Landsat TM spectral indices to create comprehensive coverages of these variables throughout the study area. By using high-resolution data, direct visual interpretation of the imagery was possible, and the resulting estimates could be used to train the lower-resolution data, providing a coverage that would not be as efficiently achieved with aerial photography or TM alone.

2.3.3.2 Spectral resolution

Increasing the number of spectral bands would seem to be an obvious way to improve prediction of forest attributes. Hyper-spectral sensors

expand on the capabilities of sensors like Landsat TM by replacing their few broad spectral bands with many narrow spectral bands (Niemann and Goodenough, Chapter 17). The motivation for this modification is the assumption that improved identification of particular spectral features will lead to improved discrimination of cover attributes. This assumption has been supported for the problem of the identification of mineral composition (Van Der Meer 1994), and specific features of canopy chemistry (Martin and Aber 1997; Zagolski et al. 1996), but not yet for remote sensing of forest structural attributes. Lefsky et al. (2001) found than AVIRIS hyperspectral images did poorly with respect to predicting forest structural attributes. This result, while tentative, can be explained by the relatively high level of correlation between the reflectance at closely spaced wavelengths, and the spectral simplicity of most forested scenes.

2.3.4   Temporal resolution

While temporal resolution might seem applicable only to change detection studies, multiple images from the same growing season have increased potential to detect forest structural attributes. For forest structural attributes such as basal area, biomass, and foliage biomass, Lefsky et al. (2001) found substantial increases in predictive power were obtained using a multi-temporal Landsat TM dataset (six images from a single growing season) in comparison to other imaging sensors, including high spatial and high spectral resolution images. The use of this sequence of images allows information on vegetation phenology to be considered (Oetter et al. 2001). It also includes images with both low and high Sun angles, which allows an indirect measure of shadow through the variable shadowing in the canopy, which is closely related to canopy height and canopy height variability (Li and Strahler 1992; Schriever and Congalton 1995).

3.   CLASSES OF IMAGERY

The discipline of remote sensing is experiencing an unprecedented period of increase in sensor numbers. However, while academic research may be increasingly concerned with these newer instruments, application work is still focused on those sensors that are established and relatively well understood. Therefore, we will focus only on these most commonly used sensors. Comprehensive reviews of currently available sensors are available in a number of texts (e.g. Kramer 2001).

In principle, any sensor can be used for any problem; for instance, it would be possible to address global land-cover using one-meter

hyperspectral imagery. If there were products that could only be created from such imagery, and if the demand for those products were great enough, then resources for such an effort might be made available. In practice there exists classes of problems that are most efficiently addressed using imagery with certain data characteristics, and we have divided sensors into these classes for the purpose of discussion. However, it must be borne in mind that these classes only reflect dominant usage at this time, and that demand for particular data products may, in the future, reassign or blur the assignment of some sensors. (Figure 2-2).

3.1 Low resolution optical sensors

Although less often used by an individual forest manager or ecologist interested at the regional or smaller scales, these lower resolution devices have numerous advantages for regional, continental and global scale mapping (Cihlar et al., Chapter 12). Many of the existing vegetation data products have been have and continue to be created using this data type, and their potential and limitations should be understood. In addition, numerous techniques used with data of higher spatial resolution were first developed for AVHRR applications, an important piece of context to bear in mind.

3.1.1 Advanced Very High Resolution Radiometer (AVHRR)

Although designed by NOAA as a weather satellite, AVHRR has seen extensive use in wide area land-cover and biophysical mapping at its intrinsic spatial resolution of 1.1 km, and resampled resolutions up to 16 km. Most often the data used in such studies are vegetation indices created from the red and near-infrared bands (Tucker 1996), in fact the vegetation index approach first saw widespread use in the interpretation of AVHRR data. The high temporal resolution of this sensor, which has a repeat interval that can provide two observations per day, has promoted the development of creating cloud-free scenes through taking maximum NDVI in a period (often bi-weekly), and the use of multi-temporal datasets for land-cover classification. Currently, high quality radiometrically corrected dataset are readily available (e.g. the Pathfinder Datasets, including an 8 km resolution product, available globally from 1981-1986). AVHRR data have been used for monitoring vegetation productivity (Tucker et al. 1980), herbaceous biomass (Tucker et al. 1983), and a variety of other ecological phenomena (Loveland 1991; Tucker 1996; Moisen and Edwards 1999).
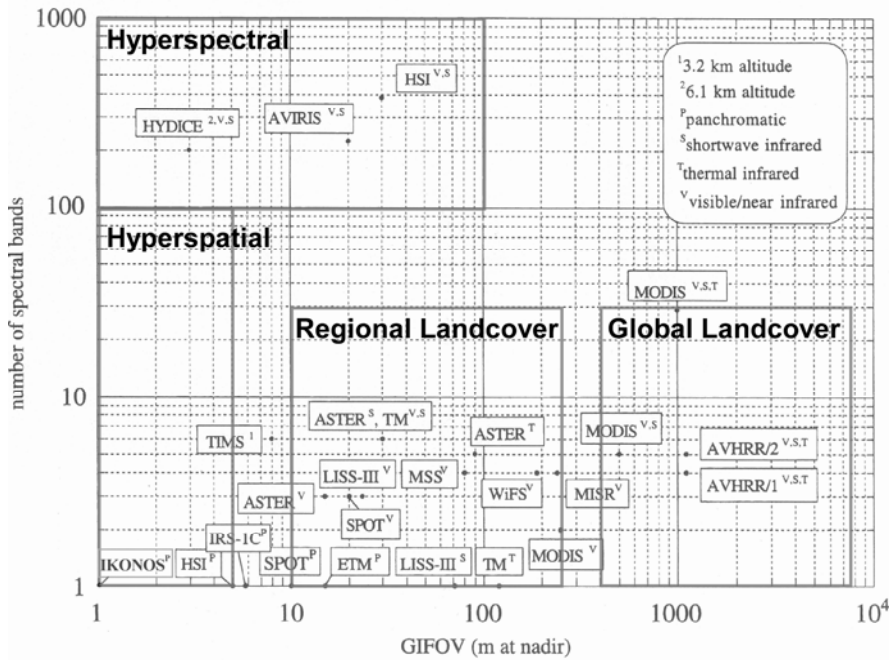
Figure 2-2. Diagram of commonly used sensors, plotted in a space formed by their ground-projected instantaneous field of view (GIFOV, i.e. pixel size) and number of spatial bands. The boundaries of the four sensors types used in the text are indicated. Adapted from Schowengerdt (1997) with permission.

One technique of direct interest to forest ecologists and managers is the method of combining two different classes of imagery, in this case, AVHRR and Landsat TM, to map an attribute of interest. In these studies (Iverson et al. 1989; Zhu and Evans 1992), a subset of TM images for the study area were classified into timberland or non-timberland and then the fraction of each of the 30 m TM pixels within each AVHHR pixel was calculated. Regressions were then performed between the TM estimate of percent timberland and indices derived from the AVHRR image to provide wide area coverage of forest cover. Starting with Townsend et al. (1985), classification of NDVI trajectories for the growing season (calculated using AVHRR) have also been used extensively for land cover classification (Loveland 1991).

3.1.2   Moderate resolution Imaging Spectrometer (MODIS)

Partially in response to the utility of devices like AVHRR, MODIS was designed as a low to moderate resolution sensor to address question

concerning land surface processes, atmospheric water vapor, clouds and aerosol monitoring, ocean color, phytoplankton and biogeochemistry, and temperatures of the surface and clouds (Masuoka et al. 1998; Justice et al. 1998). In contrast to AVHRR, which has two bands of interest for vegetation mapping, MODIS has at least 7 (Colour Plate 1) suitable for vegetation studies. Whereas AVHRR had a resolution of 1.1 km, MODIS data has variable spatial resolution in each band, including 250 m resolution bands in the red and near-infrared, 500 m bands for blue, green, and middle infrared, and 1000 m in the visible and near infrared. MODIS, the instrument, is currently flying on the Terra spacecraft; a second satellite, Aqua (EOS PM) was launched in the spring of 2002, with the same model of MODIS sensor (among others) on board. The temporal resolution of MODIS data is currently 1-2 days, when Aqua is operation, the interval will be half that.

A unique feature of the MODIS program is the time and effort spent of algorithm development for the sensor. In addition to the raw data typically provided from a sensor, the MODIS datasets include radiometrically corrected reflectance (Colour Plate 2A & B), vegetation indices, leaf area index (Colour Plate 2C), land cover and land cover change, and even a model based estimate of NPP (Running et al. 1994). While these products will require extensive validation (Cohen and Justice 1999), and may not be relevant for some individual's purposes, many researchers will find them useful as, at least, inputs for intermediate steps in the creation of data products.

3.2   Moderate resolution optical satellites

For all the variety in sensors available to the remote sensing analyst today, the majority of digital image processing for terrestrial projects is still being done with this class of instruments, and with one of two families of sensors: Landsat TM and SPOT. In our opinion, this reflects the general utility of these devices, rather than the timidity of the remote sensing community. Each strikes a balance between spatial, spectral and temporal resolution that has met the needs of land managers and scientists for (in the case of Landsat) the last three decades.

3.2.1   Multispectral Scanner (MSS), Thematic Mapper (TM), and Enhanced Thematic Mapper Plus (ETM+)

Launched in July of 1972, Landsat 1 carried two instruments, the Return Beam Vidicon (eliminated after the launch of Landsat 3 in 1978) and the Multispectral Scanner, (eliminated after the launch of Landsat 5 in 1984). Few people today use the Return Beam Vidicon data, so we will focus on

MSS. MSS had four principal bands: green, red and two bands in the near-infrared. A fifth band in the thermal was added for Landsat 3, then subsequently removed. The pixel size of MSS is source of some confusion: the IFOV of the pixels is 79.5 m (81.5 m in Landsat 4 and 82.5 m in Landsat 5), but the pixel size in the cross-track direction is over-sampled to 56.5 m. While MSS has been distributed with the 56.5 x 79.5 m pixel size, it is also routinely resampled to a 60 x 60 m pixel size for distribution. MSS data has relatively low radiometric resolution, 7 bits for the first three bands (green, red, and the first near-infrared) and 6 bits for the second near-infrared band. Although MSS is no longer part of the Landsat complement of sensors, it is still in use for historic and change-detection studies (Cohen et al. 1996).

TM was first included on Landsat 4, launched in 1982. It contains seven bands (Colour Plate 1) including red, green, blue, near-infrared, two mid-infrared and a thermal band. Pixel size is 28.5 meters in all bands except the thermal (120m). The sensor design allows each pixel to be observed for a longer period then in the MSS, which allows smaller pixel size and 8-bit resolution. Improvements in ETM+, launched on Landsat 7 in 1999, include the addition of a 15 m panchromatic band, and improved spatial resolution (60 M) on the thermal band. Early Landsat satellites (1-3) had a revisit interval of 18 days; later satellites had orbits with a revisit interval of 16 days. MSS, TM and ETM+ all have an image size of 185 km x 185 km. Colour Plate 2D presents a single tasseled cap transformed TM image from the H.J. Andrews Experimental forest on the western slope of the Cascade range in Oregon. Colour Plate 2E shows the first three principal components from a 6-image stack of tasseled cap images for the same area, as described in Lefsky et al. (2001).

3.2.2   Systeme Pour d'Observation de la Terre (SPOT)

The French SPOT system was first launched in 1986, and a total of four satellites with three different sensors have been launched. The earliest device, the HRV, is similar to Landsat MSS in spectral resolution, consisting of green, red, and near-infrared bands. It has a narrower swath (60 km vs. MSS 185 km), but higher spatial resolution (20 m vs MSS 56 x 79 m). It can also work in a panchromatic mode to achieve 10 x 10 m resolution – a significant achievement in 1984. SPOT 4 carries an updated HRVIR instrument that adds a mid-infrared band to allow some of the TM capabilities dependent on that spectral range, such as the tasseled cap wetness index.

3.3   **High spatial resolution sensors**

Although there are many sources of high spatial resolution (hyperspatial) imagery, we will focus on the two digital technologies: digital frame cameras and high-resolution satellites. Aerial photography has already been discussed in section 2.3.2.

Digital frame cameras replace the film in a conventional camera with a solid-state array of imaging elements. Because of similarity of the two systems, much of what is known about aerial photographs can be directly applied to DFCs. The use of DFC's allows real time viewing of results, eliminates film processing and printing charges, and the errors associated with scanning conventional photographs or transparencies. Unlike similar line-imager devices, each pixel in the DFC image is acquired simultaneously, which simplifies geo-rectification. Current sensor arrays (as in the ADAR 5000/5500) result in narrower swath widths than conventional aerial photographs, and are generally flown with a spatial resolution of about 1 m, but can be flown at higher resolutions at the expense of even narrower swath width. With projected improvements in the sensor arrays, it has been estimated that the data from DFC's will replace conventional aerial photographs for many applications (Pitt et al. 1997). Colour Plate 2F shows data from the ADAR 5500 from the H.J. Andrews Experimental Forest. Colour Plate 2G shows the area within the yellow box in Colour Plate 2F.

High-resolution satellites, such as the IKONOS system, have recently become available for commercial use. The IKONOS system, launched in September 1999, offers images with high spatial resolution (1m panchromatic, 4 m multispectral [R, G, B, NIR] – See Colour Plate 1) that are geo-rectified to one of two levels of precision. The IKONOS system can, for an additional fee, be "special-tasked" to an area to acquire images within a seven-day period. A sensor with even higher spatial resolution, Quickbird, was launched in October 2001, with 0.61 m resolution in the panchromatic, and 2.44 m resolution for multispectral [R, G, B, NIR] images.

Aerial photography and digital frame cameras are airborne sensors which will allow for the most flexibility in planning deployments; however selection of an airborne sensor will demand that some time be devoted to plan and coordinate contracting for collection of images. Of the two airborne sensors, aerial photographs have superior spatial resolution, and can be analyzed without being scanned and geo-rectified, which may save time in analysis. If it will be necessary to directly manipulate the image data, digital frame cameras have the advantage of providing a digital product, without the errors associated with the scanning process. However, it should be noted that data collected from unrectified aerial photographs is often successfully incorporated into a GIS framework through simple visual comparison of

features on the photos to existing rectified images, and subsequent on-screen digitization. The chief advantage of using data from high-resolution satellites is that they are available "off the shelf", and will require minimal planning. However, as with 1m DFC imagery, their spatial resolution is still relatively coarse for some analyses typically done with aerial photography (Pitt et al. 1997; Culvenor, Chapter 9).

3.4   Hyperspectral sensors

The sensors discussed so far are multispectral – wherein they record a small number of spectral bands that represent relatively wide spectral ranges. Multispectral sensors are one strategy for obtaining spectral data. To efficiently record most variation, they break the spectra into a few bands where there are significant differences between the spectra of a wide range of materials. The process inevitably results in compromises, as a good band interval for one application may not suit another. As technology improved and more data could be recorded, hyperspectral sensors were developed. These sensors record many (often more than 200 as in AVIRIS – See Colour Plate 1) narrow bands, and avoid the errors introduced by low spectral resolution (Niemann and Goodenough, Chapter 17). Although these sensors have been in the commercial market, and satellite systems are being worked on, they are more costly and more difficult to obtain then satellite images or *hyperspatial* images. The spectral resolution of one of these sensors is impossible to capture in the three bands available in the print medium, Colour Plate 2H and 4J present the first (1-3) and second (4-6) set of three principal components of an AVIRIS image collected at the H.J. Andrews Experimental Forest. Richards and Jia (1999) detail the features of six popular airborne hyperspectral sensors.

3.5   SAR sensors

There are currently three operational satellite SAR systems, the European ERS-1 and ERS-2, and the Canadian Radarsat. The ERS satellites, launched in 1991 and 1995, operate in the C band with a single (VV) polarization, and cover a 100 km wide swath with 30 m pixels. Although the ERS satellites were primarily designed for oceanographic applications, these also have seen wide use on land. Radarsat is the more versatile of these satellites, with one standard and six non-standard modes, all with a C band, HH polarization signal. Incidence angles can range from 19 to 49 degrees, and swath widths from 50 to 500 km. Cross-track (or range) resolution is 27 m while along-track (azimuth) resolution varies from 19-24 m. Either satellite can be used for interferometry, with some limitations (Baltzer 2001).

There are also a number of airborne radar systems that have potential for use in remote sensing of forests. TOPSAR, developed by NASA's Jet Propulsion Laboratory (JPL), was designed as a topographic mapping sensor by radar interferometry, and can collect multi-polarization data in the L, P and C bands. As mentioned before, the coherence between the two interferometric return signals has been used to estimate vegetation height (Rodriguez and Martin 1992). Typical swath width is 10 km. GEOSAR, developed by JPL, the California Department of Conservation, and Calgis, Inc, is another device designed for interferometric mapping of topography, that could also provide multi-polarization data in the X and P bands, over a 20 km wide swath (Hensley et al. 1999).

3.6   **Lidar sensors**

Discrete-return lidar has become a growth area for both specialized remote sensing suppliers, as well as larger surveying and photogrammetry firms (Flood and Gutelis 1997). The primary customers of these firms are municipalities, developers and natural resource managers seeking a relatively low cost alternative to traditional surveying to provide high resolution topographic maps and digital terrain models (DTM), or companies looking for rapid methods to survey utility right-of-ways. While these firms are making lidar remote sensing more available, their systems are designed and operated with the needs of their primary customers in mind. Therefore, a careful consideration of the sensor configuration and post-processing techniques must be made with project goals in mind. Numerous different discrete-return systems are available; for a detailed technical review of these sensors, see Wehr and Lohr (1999). A directory of sensors and lidar remote sensing firms can be found in Baltsavias (1999).

4.   **MATCHING IMAGERY WITH APPLICATIONS**

When thinking about the attributes of the forest that we want to remotely sense, it becomes clear that there are several broad classes of attributes that share related mechanisms of, and limitations on, their remote estimation. For instance, the mechanisms involved in the remote sensing of canopy cover, absorbed photosynthetically active radiation (F_{APAR}), and leaf area index (LAI) are going to be similar, although the formal definition of these attributes, and their estimation in the field, can be quite different. For the purposes of this discussion, we have defined classes of attributes related to: canopy cover, stand structure, stand composition, and disturbance. Each class is defined by the commonality among the attributes themselves, by the

aspect of canopy structure that they are related to, and by the way that aspect of canopy structure modifies the quantity and quality of electromagnetic radiation.

4.1   Attributes related to canopy cover

These attributes, which include foliage or canopy cover, F_{APAR}, and leaf area index, have the clearest link with the aspects of the physical organization of the canopy that remote sensing can most easily measure. In conventional optical imagery, such as aerial photos, Landsat ETM+, or SPOT HRV, reflected energy from the canopy and background surfaces mix in a roughly linear fashion, so that if there is 50% canopy cover, then 50% of the signal returned to the sensor will be from foliage, and 50% from the other cover components, such as bare soil, rock, and ground vegetation. Increasing canopy cover will be indicated by decreased reflectance in the visible (especially red) wavelengths (darker tones on aerial photography), due to the high absorptance of foliage in this spectral range. At the same time, foliage is highly reflective in the near-infrared, so that increasing foliage does not affect brightness in this region as much.

Numerous indices ((Normalized Difference Vegetation Index (Tucker 1979), Tasseled Cap Greenness (Crist and Cicone 1983), Simple Ratio (Spanner et al. 1994)) exploit the continuous spectral difference to distinguish between high and low canopy cover (Asner et al., Chapter 8). Any one of these indices can do a reasonable job of predicting a variable like canopy cover or F_{APAR}. One variable that is more difficult to predict, and which has received a lot of attention from the remote sensing community, is LAI. LAI can be considered as the number of layers of leaves that occur above a single point on the forest floor (for details, see Fournier et al., Chapter 4). In forests, LAI can be expected to vary from 0 to 10 and occasionally even higher. Although LAI is a desirable variable for biogeochemical models, the relationship between it and cover is asymptotic; with each additional layer of leaves the amount of additional cover becomes smaller, so that after a leaf area index of 4-6, the additional layers of leaves have little effect on cover. Because changes in reflectance are being driven mostly by the change in cover, the relationship between reflectance (and reflectance derived indices) and LAI is also asymptotic (Sader et al. 1990; Spanner et al. 1990; Chen and Cihlar 1996).

Microwave sensors have also been evaluated for the estimation of cover and LAI, despite their problems with moisture on the leaf surfaces leading to variations in the dielectric constant (Sader 1987). In addition, the horizontal orientation of leaves has been a problem in estimation of LAI in deciduous canopies. However, in needle-leaf coniferous canopies, SAR systems have

been able to assess LAI up to values of 4 (Franklin et al. 1994, Ulaby and Dobson 1993).

Estimates of canopy cover have been made using both discrete-return and waveform-sampling lidar sensors. These estimates are made using the fraction of the lidar measurements considered to have been returned from the ground surface (Nelson et al. 1984; Ritchie et al. 1992, 1995, 1996; Means et al. 1999) where the measurements are the number of discrete returns, or the integrated power of a waveform. In most cases, a scaling factor (implicit or explicit) is needed to correct for the relative reflectance of ground and canopy surfaces at the wavelength of the laser (Harding et al. 2001). In these measurements, the definition of the ground surface is a critical aspect of cover determination. If the number or power of the measurements assigned to the ground return are overestimated (i.e., the elevation of the ground surface is overestimated) cover will be underestimated, and vice versa. Lefsky et al. (1999b) reported on a novel technique to estimate LAI in temperate coniferous forests, using measurements of canopy volume from a waveform recording lidar. However, this result has yet to be examined in other ecosystems.

4.2   Attributes related to canopy height

The next group of variables are related to the mean and variability of canopy height. These include tree volume, aboveground biomass, basal area, mean diameter-at-breast-height (DBH), stem density and stand age. Again, the formal definition of these attributes, and their estimation in the field, are quite variable. One variable, age, does not seem to belong at all. However, since age itself cannot be directly sensed, it is most often predicted from variables that are related to height and its variability.

Change in these attributes during the early stages of stand development can be estimated using the same cover-related spectral patterns described above, during the period in which change in vegetation cover is rising with vegetation biomass. However, with the exception of very low productivity stands, canopy closure occurs early on in most stands, while height and other attributes continue to change. Trees continue to grow in height for much of their individual lifetimes without dramatic spectral changes at the leaf level. However the spatial organization of the forest does change, as the size of the average dominant or co-dominant crown increases. Furthermore, the development of patch-scale dynamics, as the initial cohort of trees dies and younger trees take their place, means that the canopy's structure keeps changing long after the oldest trees die. This increasing variability is a sign of older stands in many forest types and can be seen in optical imagery as the presence of increasing shadow.

Accurate estimation of height-related variables is one of the most difficult tasks in the remote sensing of forests, especially in moderate to high biomass forests. Passive optical and active microwave sensors can predict these variable well in the first stages of stand development, but at moderate and high levels of biomass or volume they have poor discrimination or none at all. In a summary of research on SAR systems, Waring et al. (1995) stated that single-band systems with a single polarity had a detection limit of 150 Mg ha^{-1} for biomass and that even a combination of bands and polarizations would reach their limit at 250 Mg ha^{-1}. Similar results pertain for optical remote sensing (Sader et al. 1989; Hyppa et al. 1998; Lefsky et al. 2001). Nevertheless, for monitoring the first stages of forest development, managed stands with a short rotation age, or forests with naturally low biomass, microwave and optical systems can be effective. In some conifer forests (in particular Douglas-Fir / western hemlock) the observable aspects of canopy structure continue to change throughout stand development, and prediction of height, and its relative variables (such as aboveground biomass and in some cases, age) are more successful. These aspects of canopy structure can include trees of large stature, deep shadow, snags and dead wood in the canopy, and extensive colonization of the canopy by lichens.

It is becoming widely accepted that lidar sensors have a capacity for measuring height related attributes, including volume and aboveground biomass, to a greater degree than any other sensor type. Studies involving both discrete-return and waveform-record sensors have had success measuring height (Nelson et al. 1988), volume (Maclean and Krabill 1986), biomass (Lefsky et al. 1999a; Lefsky et al. 1999b; Drake et al. 2002), and basal area (Lefsky et al. 1999a, 1999b). These studies have involved deciduous (Lefsky et al. 1999a; Drake et al. 2002), coniferous (Nelson et al. 1988; Nilsson 1996; Naesset 1997; Lefsky et al. 1999b) and mixed (Maclean and Krabill 1986) stands in boreal (Naesset 1997; Nilsson 1996), temperate (Maclean and Krabill 1986; Nelson et al. 1988; Lefsky et al. 1999a, 1999b) and tropical sites (Nelson et al. 1997; Drake et al. 2002)**.** While lidar currently remains one of the more expensive remote sensing datasets to obtain, the increasing use of this technology for land surveying may bring down costs. In addition, analyses pairing lidar with either optical (Hudak et al. 2002) or interferometric SAR (Rodriguez et al. 2002) may result in a lower cost alternative to comprehensive lidar coverage.

4.3   Composition attributes

Attributes related to composition are the most difficult set of attributes to summarize, due to the diversity of attributes themselves and the variety of spectral or other features used to predict them. Compositional attributes

include physiognomy, phenological types (deciduous vs. evergreen), species level composition, and a variety of cover type classifications. Composition can be related to the spectral qualities of the vegetation itself, vegetation cover and its pattern, and even the spectral qualities of the background that the vegetation partially obscures. This presents an inherently complicated picture, however in many forested landscapes the tasseled cap transformation can simplify the spectral qualities of a scene, by contrasting the vegetation against soil, shadow and other scene components. Although the coefficients of the tasseled cap were derived from examination of multiple MSS (Kauth and Thomas 1976), and later TM (Crist and Cicone 1983), scenes, an empirical analysis of images from forested scenes usually produces three bands that are similar to it. Therefore, it is justifiable to use this ordering of the spectral variance of a scene as a tool to understand composition.

Within the context of western Oregon, Cohen et al. (2001) found that brightness (essentially the average of the six non-thermal TM bands) is associated with soil and litter cover (soil is commonly brighter), varying proportions of vegetation cover (high cover is darker), and with the distinction between conifer and deciduous cover (conifer is darker). Greenness (the contrast between visible and infrared bands) is associated with changes in vegetation cover (similar to NDVI) and with the proportion of conifer versus hardwood. Wetness, which is a contrast between the visible and near-infrared channels and the mid-infrared bands, is associated with increasing age and crown size in conifer stands, with lower wetness in more developed stands. In western Oregon, these three simple transformed bands have been shown to explain much of the variation in vegetation cover, conifer cover, conifer crown diameter and age (Cohen et al. 2001).

Any sensor that approximates the selection of bands that Landsat offers (e.g., the HRVIR sensor on SPOT 4) should be able to duplicate these results. However, sensors that do not include the middle-infrared band may not be able to adequately represent the wetness component of the tasseled cap, which may set a lower bound on the number and kind of bands that a sensor for forestry applications should have. Setting an upper bound on the spectral information that is needed for such a sensor is more difficult. Hyperspectral sensors have been advanced as one way to get better composition information, and some results support this (Gong and Yu 1997; Martin et al. 1998). However, as pointed out earlier, most plants have very similar spectral responses, and sunlit foliage (from which the spectra will be most clear) occurs in mixture with other components of a canopy image: shadow, shadowed foliage, and background. Therefore it is unclear whether the hyperspectral approach will yield widespread advances in predicting forest composition.

4.4   Change / disturbance monitoring

Change detection involves the comparison of images from a given location at two or more points in time. One can simply compare summaries of classifications for a given area at different points in time, or can conduct a spatially explicit analysis involving direct comparisons on a pixel-by-pixel basis (Gong and Xu, Chapter 11). In the latter, and more usual case, accurate spatial registration of two or more images in required.

Optical images are the dominant type of remote sensing for change detection, and have proven to be useful for the detection of both dramatic (stand replacement disturbances, Hall et al. 1989; Cohen et al. 2001) and subtle disturbances (insect, low intensity fire, thinning (Franklin et al. 1995; Jakubauskas et al. 1990; Franklin et al. 2000). Image processing approaches developed for optical images have also been applied to SAR images (Banner and Ahern 1995), despite difficulties with the high variability in backscatter due to moisture and seasonality (Cihlar et al. 1992), and the dependence of backscatter on topography and incidence angles (Drieman 1994; Edwards and Rioux 1995). However, the development of interferometric SAR systems, especially those on space borne platforms may soon begin to supplement optical images as a source of data for change detection. The coherence measurement appears to be more stable (Baltzer 2001) than backscatter as variable for change detection analysis. No work on change detection from lidar has yet been published, but numerous groups are looking at doing change detection in height over relatively short time increments (3-10) years. It is believed that such data may provide an estimate of net primary productivity or mean annual increment of volume.

5.   CONCLUSION – SELECTING A SOURCE OF IMAGERY

Selecting a source of imagery can be a complicated process, but the first priority must be to select a data source that has a record, preferably in the peer reviewed literature, of being able to predict the attributes you are interested in, and the resolution of the dependent variables you will need. Resolution in this case refers to the number of levels you need, from a binary presence/absence (as in forest/non-forest determinations) to continuous estimates of a variable like age or aboveground biomass. Increasing resolution in the dependent variable requires a higher level of correlation between the imagery and the dependent variable. For example, accurately distinguishing, with a given confidence, three classes of an attribute requires

a lower level of correlation between the attribute and the data source than does distinguishing ten classes or estimating that attribute continuously.

We have reviewed four classes of forest attributes and their ability to be predicted from various imagery types. Variables related to canopy cover will, in the absence of overwhelming cloud cover problems, usually be predicted from optical imagery; the option of using microwave data in this instance will require more complex processing, but is capable of making some of the same measurements, particularly in coniferous canopies. Optical sensors of any spatial resolution are appropriate for cover-like measurements, and hyperspectral data may offer some benefits by being able to use only those narrow spectral regions with the highest contrast, but multispectral data should do an adequate job.

Stand structure can be successfully estimated from optical and microwave sensors, up to relatively low levels of plant biomass. Therefore, if one's study area is predominately low biomass forest, or you only need a few classes of structure, they can be useful. If detailed estimates of forest structure are required in a high biomass study area, lidar will provide the best results. However, for study areas greater than a few tens of km^2 lidar, it is currently too expensive (~US\$ 500 / km^2) for many studies.

For general land and forest cover classification, the same caveat used above still holds; unless you have overwhelming cloud cover problems you will probably want to use optical remote sensing. Again, data of many spatial resolutions can be used for these applications, and there is also a good case for hyperspectral data for these applications. One caveat for *hyperspatial* data that bears repeating is that, if individual trees fall in multiple pixels, each pixel may be in one of several classes (shadow or sunlit, young foliage or old), requiring a detailed analysis to retrieve common land-use classes.

For change detection, hyperspectral data does not offer any obvious improvements over multispectral data – the types of change commonly being mapped are related to differences in canopy cover, which is well within a multispectral sensor's ability to describe. High spatial resolution data could have some interesting applications for change detection – but precisely matching images from two dates becomes more difficult as pixel sizes decrease. Low spatial resolution devices will almost always contain changed and unchanged area in a large pixels, although the MODIS device will produce a 250 m change detection product for global monitoring of land cover change hotspots. The 250 m resolution probably represents an upper limit for accurate change detection and, for most studies, one of the moderate resolution optical sensors would be preferable.

Finally, we believe that our review of sensors for forestry applications strongly suggests that the "best" sensor is often more than one sensor.

Whether the combination is high-resolution and lower-resolution (as in Cohen et al. 2001; or Zhu and Evans 1992), multi- and hyper-spectral (Ranchin and Wald 2000), or conventional optical and lidar (Hudak et al. 2002), the motivation is the same – combining the strengths of two or more sensors to create a solution that is tailored for the application being considered. Recognizing the individual strengths and weaknesses of each type of sensor is the first step towards applications that properly use them.

REFERENCES

Abrams, M. J., Kahle, A. B., Palluconi, F. D., & Schieldge, J. P. (1984). Geologic mapping using thermal images. *Remote Sensing of Environment,* 16, 13-33.

Asner, G. P., Braswell, B. H. Schimel, D. S., & Wessman, C. (1998). Ecological research needs from multiangle remote sensing data. *Remote Sensing of Environment,* 63, 155-165.

Bachman, C. G. (1979). *Laser Radar Systems and Techniques*. Artech House, MA.

Baltsavias, E. P. (1999). Airborne laser scanning: existing systems and firms and other resources. *ISPRS Journal of Photogrammetry & Remote Sensing,* 54, 164-198.

Baltzer, H. (2001) Forest mapping and monitoring with interferometric synthetic aperture radar (InSAR). *Progress in Physical Geography,* 25, 159-177.

Banner, A. V., & Ahern, F. J. (1995). Incidence angle effects on the interpretability of forest clearcuts using airborne C-HH SAR imagery. *Canadian Journal of Remote Sensing,* 21, 64-66.

Brock, J. C., & Wright, C. W. (2000). Preliminary results from a NASA Experimental Advanced Airborne Research LIDAR (EAARL) survey of Pacific Reef in Biscayne National Park, Florida. *Proc. 9th International Coral Reef Symposium*, 233. USGS Center For Coastal Geology, Florida.

Chauhan, N. S. (1997). Soil Moisture Estimation Under a Vegetation Cover: Combined Active Passive Microwave Remote Sensing Approach. *International Journal of Remote Sensing,* 18, 1079-1097.

Chen, J. M., & Cihlar, J. (1996). Retrieving leaf area index of boreal conifer forests using Landsat TM images. *Remote Sensing of Environment*, 55, 153-162.

Cihlar, J., Pultz, T. J., & Gray, A. L. (1992). Change detection with synthetic aperture radar. *International Journal of Remote Sensing,* 13, 401-414.

Cohen, W., Harmon, M.,Wallin, D., & Fiorella, M. (1996). Two decades of carbon flux from forests of the Pacific Northwest. *Bioscience,* 46, 836-844.

Cohen, W. B., Spies, T. A., & Fiorella, M. (1995). Estimating the age and structure of forests in a multi-ownership landscape of western Oregon, U.S.A. *International Journal of Remote Sensing,* 16, 721-746.

Cohen, W., & Justice, C. (1999). Validating MODIS terrestrial ecology products: linking in situ and satellite measurements. *Remote Sensing of Environment,* 70, 1-3.

Cohen, W. B., Maiersperger, T. K., Spies, T. T. A., & Oetter., D. R. (2001). Modeling Forest Cover Attributes as Continuous Variables in a Regional Context with Thematic Mapper Data. *International Journal of Remote Sensing,* 22, 2279-2310.

Crist, E. P., & Cicone., R. C. (1983). Investigations of thematic mapper data dimensionality and features using field spectrometer data. *Proc. Seventeenth Int. Symp. Remote Sensing of Environment*, 3. Environ. Res. Inst. Michigan, Ann Arbor MI, 9-13 May.

Dobson, M. C., Pierce, L., Sarabandi, K., Ulaby, F. T., & Sharik, T. (1992). Preliminary analysis of ERS-SAR for forest ecosystem studies. *IEEE Transactions on Geoscience and Remote Sensing,* 30, 412-415.

Drake, J. B., Dubayah, R. O., Clark, D. B., Knox, R. G., Blair, J. B., Hofton, M. A., Chazdon, R. L., Weishample, J. F., & Prince, S. (2001). Estimation of Tropical Forest Structural Characteristics using Large-footprint Lidar. *Remote Sensing of Environment,* 79, 305-319.

Drieman, J. A. (1994). Forest cover typing and clearcut mapping in Newfoundland with C-band SAR. *Canadian Journal of Remote Sensing,* 20, 11-16.

Edwards, G., & Rioux, S. (1995). A detailed assessment of relative displacement error in cutover boundaries derived from airborne C-band SAR. *Canadian Journal of Remote Sensing,* 21, 185-197.

Eineder, M., Bamler, R., Adam, N., Suchandt, S., & Breit, H. (2000). Analysis of SRTM Interferometric X-Band Data: First Results. *Proceedings of the International Geoscience and Remote Sensing Symposium 2000*, 6, 2593-2595. Honolulu, Hawaii.

Eppler, D. T., & Farmer, L. D. (1991). Texture analysis of radiometric signatures of new sea ice forming in Arctic lands. *IEEE Transactions on Geoscience and Remote Sensing,* 29, 233-241.

Flood, M., & Gutelis, B. (1997). Commercial implications of topographic terrain mapping using scanning airborne laser radar. *Photogrammetric Engineering and Remote Sensing,* 63, 327-366.

Franklin, S. E., Lavigne, M. B., Wilson, B. A., & Hunt, E. R. (1994). Empirical relations between balsam fir (*Abies balsamea*) forest stand conditions and ERS-1 SAR data in western Newfoundland. *Canadian Journal of Remote Sensing,* 20, 124-130.

Franklin, S. E., Bowers, W. W., & Ghitter, G. (1995). Discrimination of adelgid-damage on single balsam fir trees with aerial remote sensing data. *International Journal of Remote Sensing,* 16, 2779-2794.

Franklin, S. E., Moskal, L. M., Lavinge, M. B., & Pugh, K. (2000). Interpretation and classification of partially harvested forest stands in the Fundy Model Forest using multitemporal Landsat TM. *Canadian Journal of Remote Sensing*, 26, 318-333.

Gates, D. M., & Tantraporn W. (1952). The reflectivity of deciduous trees and herbaceous plants in the infrared to 25 microns. *Science,* 115, 613-616.

Gong, P., Pu, R., &Yu, B. (1997). Conifer species recognition: an exploratory analysis of in situ hyperspectral data. *Remote Sensing of Environment,* 62, 189-200.

Hall, R. J., Kruger, A. R., Scheffer, J., Titus, S. J., & Moore, W. C. (1989). A statistical evaluation of Landsat TM and MSS for mapping forest cutovers. *Forest Chronicle*, 65, 441-449.

Harding, D. J., Lefsky, M. A., & Parker, G. G. (2001). Lidar altimeter measurements of canopy structure: methods and validation for closed-canopy broadleaf forest. *Remote Sensing of the Environment,* 76, 283-297.

Hensley, S., Chapin, E., & Bartman, R. K. (1999). Baseline Calibration Of The Geosar Interferometric Mapping Instrument. *Presented at the Committee on Earth Observing Satellites*. Toulouse, France. October 1999.

Hudak, A. T., Lefsky, M. A., Cohen, W. B., & Berterretche, M. (2002). Integration of lidar and Landsat ETM+ data for estimating and mapping forest canopy height. *Remote Sensing of Environment*, 82, 398-417.

Hyppa, J., Huuppa, H., Inkinen, M., & Engdahl, M. (1998). Verification of the potential of various remote sensing data sources for forest inventory. *Proceedings of IEEE Geosciences and Remote Sensing Society*, 1812-1814. July 6-10, 1998, Seattle Washington. IEEE, Piscataway, NJ.

Iverson, L. R., Cook, E. A., & Graham, R. L. (1989). A technique for extrapolating and validating forest cover across large regions: Calibrating AVHRR data with TM data. *International Journal of Remote Sensing,* 10, 1805-1812.

Jakubauskas, M. E, Lulla, K. P., & Mausel, P. W. (1990). Assessment of vegetation change in a fire-altered forest landscape. *Photogrammetric Engineering and Remote Sensing*, 56, 371-377.

Justice, C., Vermote, E., Townshend, J., DeFries, R., Roy, D., Hall, D., Salomonson, V., Privette, J., Riggs, G., Strahler, A., Lucht, W., Myneni, R., Knyazikhin, Y., Running, S., Nemani, R., Wan, Z., Huete, A., van Leeuwen, W., Wolfe, R., Giglio, L., Muller, J.-P., Lewis, P., & Barnsley, M. (1998). The Moderate Resolution Imaging Spectroradiometer (MODIS): land remote sensing for global change research. *IEEE Transactions on Geoscience and Remote Sensing,* 36, 1228-1249.

Kasischke, E. S., Bourgeau-Chavez, L. L., Christensen, N. L., & Haney, E. (1994). Observations on the sensitivity of ERS-1 SAR image intensity to changes in aboveground biomass in young loblolly pine forests. *International Journal of Remote Sensing,* 15, 3-16.

Kauth, R. J., & Thomas, G. S. (1976). The tasseled cap--A graphic description of the spectral-temporal development of agricultural crops as seen by Landsat. *Proc. Second Ann. Symp. Machine Processing of Remotely Sensed Data.* Purdue U. Lab. App. Remote Sens., West Lafayette IN, 6 June-2 July.

Kimes, D. S., Kerber, A. G., & Sellers, P. J. (1993). Spatial averaging errors in creating hemispherical reflectance (albedo) maps from directional reflectance data. *Remote Sensing of Environment,* 45, 85-94.

Kramer, H. J. (2001*). Observation of the earth and its environment: survey of missions and sensors* (4th ed.). Springer-Verlag, Berlin.

Lefsky, M. A., Harding, D., Cohen, W. B., & Parker, G. G. (1999a). Surface lidar remote sensing of basal area and biomass in deciduous forests of eastern Maryland, USA. *Remote Sensing of the Environment,* 67, 83-98.

Lefsky, M. A., Cohen, W. B., Acker, S. A., Spies, T. A., Parker, G. G., & Harding, D. (1999b). Lidar remote sensing of biophysical properties and canopy structure of forest of Douglas-fir and western hemlock. *Remote Sensing of Environment,* 70, 339-361.

Lefsky, M. A., Cohen, W. B., & Spies, T. A. (2001). An evaluation of alternate remote sensing products for forest inventory, monitoring, and mapping in Douglas-fir forests of western Oregon. *Canadian Journal of Forest Research,* 31, 78-87.

Lefsky, M. A., Cohen, W. B., Parker, G. G., & Harding, D. J. (2002). Lidar remote sensing for ecosystem studies. *Bioscience,* 52, 19-30.

Li, X., & Strahler, A. H. (1992). Geometric-optical bidirectional reflectance modeling of the discrete crown vegetation canopy: Effect of crown shape and mutual shadowing. *IEEE Transactions on Geoscience and Remote Sensing,* 30, 276-292.

Lillesand, T. M., & Kiefer, R. W. (2000). *Remote sensing and image interpretation.* John Wiley and Sons, New York.

Loveland, T. R., Merchant, J. W., Ohlen, D. O., & Brown, J. F. (1991). Development of a land-cover characteristics database for the conterminous U.S. *Photogrammetric Engineering & Remote Sensing,* 57, 1453-1463.

Luckman, A., Baker, J., Honzak, M., & Lucas, R. (1998). Tropical forest biomass density estimation using JERS-1 SAR: seasonal variation, confidence limits, and application to image mosaics. *Remote Sensing of Environment,* 63, 126-139.

Luvall, J. C., & Holbo, H. R. (1991). Thermal remote sensing methods in landscape ecology. Turner, M. G., & RGardner, R. H. (Eds.). *Quantitative Methods in Landscape Ecology,* 127-152. Springer-Verlag, New York NY.

Maclean, G. A., & Krabill, W. B. (1986). Gross-merchantable timber volume estimation using an airborne LIDAR system. *Canadian Journal of Remote Sensing,* 12, 7-18.

Martin, M., & Aber, J. (1997). High spectral resolution remote sensing of forest canopy lignin, nitrogen, and ecosystem processes. *Ecological Applications,* 7, 431-443.

Martin, M., Newman, S., Aber, L., & Congalton, R. (1998). Determining forest species composition using high resolution remote sensing data. *Remote Sensing of Environment,* 65, 249-254.

Masuoka, E., Fleig, A., Wolfe, R., & Patt, F. (1998). Key characteristics of MODIS data products. *IEEE Transactions on Geoscience and Remote Sensing,* 36, 1313-1323.

Means, J. E., Acker, S. A., Harding, D. J., Blair, J. B., Lefsky, M. A., Cohen, W. B., Harmon, M., & McKee, W. A. (1999). Use of large-footprint scanning airborne lidar to estimate forest stand characteristics in the western Cascades of Oregon. *Remote Sensing of the Environment,* 67, 298-308.

Moisen, G., & Edwards, T. C., Jr. (1999). Use of generalized linear models and digital data in a forest inventory of northern Utah. *Journal of Agricultural, Biological, and Environmental Statistics,* 4, 372-390.

Mouginis-Mark, P. J., Garbeil, H., & Flament, P. (1994). Effects of viewing geometry on AVHRR observations of volcanic thermal anomalies. *Remote Sensing of Environment,* 48, 51-60.

Naesset, E. (1997). Determination of mean tree height of forest stands using airborne laser scanner data. *ISPRS Journal Photogrammetry and Remote Sensing,* 52, 49-56.

Nelson, R. F., Krabill, W. B., & Maclean, G. A. (1984). Determining forest canopy characteristics using airborne laser data. *Remote Sensing of Environment,* 15, 201-212.

Nelson, R. F., Krabill, W. B., & Tonelli, J. (1988). Estimating forest biomass and volume using airborne laser data. *Remote Sensing of Environment,* 24, 247-267.

Nilsson, M. (1996). Estimation of Tree Heights and Stand Volume Using an Airborne Lidar System. *Remote Sensing of Environment,* 56, 1-7.

Oetter, D., Cohen, W., Berterretche, M., Maiersperger, T., & Kennedy, R. (2001). Land cover mapping in an agricultural setting using multiseasonal Thematic Mapper data. *Remote Sensing of Environment,* 76, 139-155.

Pitt, D. G., Wagner, R. G., Hall, R. J., King, D. J., Leckie, D. G., & Runesson, U. (1997). Use of remote sensing for forest vegetation management: A problem analysis. *Forestry Chronicle,* 73, 459-477.

Ranchin, T., & Wald, L. (2000). Fusion of high spatial and spectral images: the ARSIS concept and its implementation. *Photogrammetric Engineering & Remote Sensing,* 66, 49-61.

Ranson, K. J., & Williams, D. L. (1992). Remote sensing technology for forest ecosystem analysis. Shugart, H. H., Leemans, R., & Bonan, G. B. (Eds.). *A Systems Analysis of the Global Boreal Forest*, 267-290. Cambridge U. Press, New York NY.

Ranson, K. J., Irons, J. R., & Williams, D. L. (1994). Multispectral bidirectional reflectance of northern forest canopies with the advanced solid-state array spectroradiometer (ASAS). *Remote Sensing of Environment,* 47, 276-289.

Richards, J. A., & Jia, X. (1999). *Remote Sensing Digital Imagery Analysis: An Introduction.* Springer Berlin.

Rignot, E. J., & Way, J. B. (1994). Monitoring freeze-thaw cycles along north-south Alaskan transects using ERS-1 SAR. *Remote Sensing of Environment,* 49, 131-137.

Rignot, E. J., Way, J. B., McDonald, K., Viereck, L., Williams, C., Adamas, P., Payne, C., Wood, W., & Shi, J. (1994). Monitoring of environmental conditions in taiga forests using ERS-1 SAR. *Remote Sensing of Environment,* 49, 145-154.

Ritchie, J. C., Everitt, J. H., Escobar, D. E., Jackson, T. J., & Davis, M. R. (1992). Airborne laser measurements of rangeland canopy cover and distribution. *Journal of Range Management,* 45, 189-193.

Ritchie, J. C., Humes, K. S., & Weltz, M. A. (1995). Laser altimeter measurements at Walnut Gulch watershed, Arizona. *Journal of Soil and Water Conservation,* 50, 440-442.

Ritchie, J. C., Menenti, M., & Weltz, M. A. (1996). Measurements of land surface features using an airborne laser altimeter: The HAPEX-Sahel experiment. *International Journal of Remote Sensing,* 17, 3705-3724.

Rodriguez, E., & Martin, J. M. (1992). Theory and design of interferometric synthetic aperture radars. *IEEE Proceedings-F Radar and Signal Processing*, 139, 147-159.

Rodriguez, E., Michel, T.R., & Harding, D.J. 2002. Interferometric measurements of canopy height characteristics for coniferous forests, *IEEE Transactions on Geoscience and Remote Sensing,* (*In Review*)

Rosen, P.A., Hensley, S., Joughin, I. R., Li, F.K., Madsen, S.N., Rodriguez, E., & Goldstein, R.M. (2000). Synthetic aperture radar interferometry - Invited paper, *Proc. IEEE* 88, 3, 333-382.

Running, S. W., Justice, C. O., Salmonson, V., Hall, D., Barker, J., Kaufmann, Y. J., Strahler, A. H., Huete, A. R., Muller, J. –P., Vanderbilt, V., Wan, Z. M., Teillet, P., & Carneggie, D. (1994). Terrestrial remote sensing science and algorithms planned for EOS/MODIS. *International Journal of Remote Sensing,* 15, 3587-3620.

Sader, S. A. (1986). Analysis of effective radiant temperatures in a Pacific Northwest forest using thermal infrared multispectral scanner data. *Remote Sensing of Environment,* 19, 105-115.

Sader, S.A. (1987). Forest biomass, canopy structure, and species composition relationships with multipolarization L band synthetic aperture radar data. *Photogrammetric Engineering and Remote Sensing*, 53, 193-202.

Sader, S. S., Waide, R. B., Lawrence, W. T., & Joyce, A. T. (1989). Tropical forest biomass and successional age class relationships to a vegetation index derived from Landsat TM data. *Remote Sensing of Environment,* 28, 143-156.

Sader, S. A., Stone, T. A., & Joyce, A. T. (1990). Remote sensing of tropical forests: An overview of research and applications using non-photographic sensors. *Photogrammetric Engineering & Remote Sensing,* 56, 1343-1351.

Schriever, J. R., & Congalton, R. G. (1995). Evaluating seasonal variability as an aid to cover-type mapping from Landsat Thematic Mapper data in the Northeast. *Photogrammetric Engineering & Remote Sensing,* 61, 321-327.

Schowengerdt, R. A. (1997). *Remote Sensing: Models and methods for image processing*. Academic Press, San Diego, CA.

Spanner, M. A., Pierce, L. L., Peterson, D. L., & Running, S. W. (1990). Remote sensing of temperate coniferous forest leaf area index: The influence of canopy closure, understory vegetation and background reflectance. *International Journal of Remote Sensing,* 11, 95-111.

Spanner, M. A., Johnson, L., Miller, J., McCreight, R., Freemantle, J., Runyon, J., & Gong, P. (1994). Remote sensing of seasonal leaf area index across the Oregon transect. *Ecological Applications,* 4, 258-271.

Strahler, A. H., Woodcock, C. E., & Smith, J. A. (1986). On the nature of models in remote sensing. *Remote Sensing of Environment,* 20, 121-139.

Townsend, J.R.G., Goff, T. E., & Tucker, C. J. (1985). Multitemporal dimensionality of images of normalized difference vegetation index at continental scales. *IEEE Transactions on Geoscience and Remote Sensing,* 23, 888-895.

Tucker, C. J. (1979). Red and photographic infrared linear combinations for monitoring vegetation. *Remote Sensing of Environment,* 8, 127-150.

Tucker, C. J., Holben, B. N., Elgin, J. H., & McMurtrey, J. E. (1980). Relationship of spectral data to grain yield variation. *Photogrammetric Engineering & Remote Sensing,* 46, 657-666.

Tucker, C. J., Vanpraet, C., Boerwinkel, E., & Gaston, A. (1983). Satellite remote sensing of total dry matter production in the Senegalese Sahel. *Remote Sensing of Environment,* 13, 461-474.

Tucker, C. J. (1996). History of the use of AVHRR data for land applications. D'Souza, G., Belward, A. S., & Malingeau, J. P. (Eds.). *Advances in the use of NOAA AVHRR data for land applications*, 1-19. ECSC, EEC and EAEC. Brussels and Luxembourg.

Ulaby F.T., & Dobson, M. C. (1993). Radar response of vegetation: an overview. *Proceedings of the Third Spaceborne Imaging Radar Symposium,* 151-183. Jet Propulsion Lab Publications 93-16.

Van der Meer, F. (1994). Extraction of mineral absorption features from high-spectral resolution data using non-parametric geostatistical techniques. *International Journal of Remote Sensing,* 15, 2193-2214.

Vane, G., & Goetz, A. F. (1993). Terrestrial imaging spectometry: Current status, future trends. *Remote Sensing of Environment,* 44, 117-126.

Wang, Y., Kasischke, E. S., Melack, J. M., Davis, F. W., & Christensen, N. L. (1994). The effects of changes in loblolly pine biomass and soil moisture on ERS-1 SAR backscatter. *Remote Sensing of Environment,* 49, 25-31.

Waring, R. H., Way, J., Hunt, E. R., Morrissey, L., Ranson, K. J., Weishampel, J. F., Oren, R., & Franklin, S. E. (1995). Imaging radar for ecosystem studies. *BioScience,* 45, 715-723.

Way, J., Paris, J., Dobson, M., McDonald, K., Ulaby, F., Weber, J., Ustin, S., Vanderbilt, V., & Kasischke, E. (1991). Diurnal change in trees as observed by optical and microwave sensors: The EOS synergism study. *IEEE Transactions on Geoscience and Remote Sensing,* 29, 807-821.

Way, J., Rignot, E. J., McDonald, K. C., Oren, R., Kwok, R., Bonan, G., M. Dobson, M. C., L. Viereck, A., & Roth, J. E. (1994). Evaluating the type and state of Alaska taiga forests with imaging radar for use in ecosystem models. *IEEE Transactions on Geoscience and Remote Sensing,* 32, 353-370.

Wehr, A., & Lohr, U. (1999). Airborne laser scanning-an introduction and overview. *ISPRS Journal of Photogrammetry & Remote Sensing,* 54, 68-82.

Wolter, P. T., Mladenoff, D. J., Host, G. E., & Crow, T. R. (1995). Improved forest classification in the Lake States using multi-temporal Landsat imagery. *Photogrammetric Engineering & Remote Sensing,* 61, 1129-1143.

Woodcock, C. E., & Strahler, A. H. (1987). The factor of scale in remote sensing. *Remote Sensing of Environment,* 21, 311-332.

Wulder, M. (1998). Optical remote-sensing techniques for the assessment of forest inventory and biophysical parameters. *Progress in Physical Geography* 22, 449-476

Zagolski, F. P., Pinel, V., Romier, J., Alcayde, D., Fontanari, J., Gastellu-Etchegorry, J. P., Giordano, G., Marty, G., Mougin, E., & Joffre, R. (1996). Forest canopy chemistry with high spectral resolution remote sensing. *International Journal of Remote Sensing,* 17, 1107-1128.

Zhu, Z., & Evans, D. L. (1992). Mapping midsouth forest distributions. *Journal of Forestry,* 90, 27-30.